Characterization of natural illuminants in forests and the use of digital video data to reconstruct illuminant spectra

Chuan-Chin Chiao

Department of Biological Sciences, University of Maryland, Baltimore County, 1000 Hilltop Circle, Baltimore, Maryland 21250

Daniel Osorio

School of Biological Sciences, University of Sussex, Brighton BN1 9QG, UK

Misha Vorobyev and Thomas W. Cronin

Department of Biological Sciences, University of Maryland, Baltimore County, 1000 Hilltop Circle, Baltimore, Maryland 21250

Received December 16, 1999; revised manuscript received June 16, 2000; accepted June 21, 2000

We describe illumination spectra in forests and show that they can be accurately recovered from recorded digital video images. Natural illuminant spectra of 238 samples measured in temperate forests were characterized by principal-component analysis. The spectra can be accurately approximated by the mean and the first two principal components. Compared with illumination under open skies, the loci of forest illuminants are displaced toward the green region in the chromaticity plots, and unlike open sky illumination they cannot be characterized by correlated color temperature. We show that it is possible to recover illuminant spectra accurately from digital video images by a linear least-squares-fit estimation technique. The use of digital video data in spectral analysis provides a promising new approach to the studies of the spatial and temporal variation of illumination in natural scenes and the understanding of color vision in natural environments. © 2000 Optical Society of America [S0740-3232(00)02410-8]

OCIS codes: 150.2950, 300.6170, 120.5630, 040.1520, 040.7290, 330.1720.

1. INTRODUCTION

The spectral distribution of daylight has been well characterized by Judd *et al.*[1] Their analyses, based on a composite data set of daylight spectra (total of 622 samples from Rochester, N.Y.; Enfield, England; and Ottawa, Canada), show that only two characteristic vectors (eigenvectors, or principal components) and the mean spectrum are sufficient to reconstruct the spectral distribution of daylight. Their results have inspired the application of principal-component analysis (PCA) to characterize reflectance spectra.[2–5] Judd *et al.*[1] also demonstrated that the spectral distribution of daylight is fairly well characterized by correlated color temperature, which led the CIE to assign D55, D65, and D75 (correlated color temperatures 5503, 6504, and 7504 K, respectively) as standard daylight spectra.[6] Although the daylight spectra analyzed by Judd *et al.*[1] are very common light sources in natural environments, these spectra represent light only under open sky. In forests, as this light travels through layers of leaves, its spectrum would be altered.[7] Animals live in forests, so the illuminants they encounter vary with time and location. To understand physiological mechanisms of color vision and color constancy, one must study the spectral properties of illuminants in natural habitats such as forests. In the first part of this study, we measured 238 illuminant spectra in temperate forests and characterized these spectra using the methods of Judd *et al.*[1] We used these data to compare the spectral properties of daylight and forest light.

To study the spatial variation of illumination, one must measure all illuminant spectra within a given field of view simultaneously. However, it is not practical to put an array of spectroradiometers on the floors of forests and to record thousands of spectra at one time. We relied on recent developments in charge-coupled devices (CCD) to reconstruct the required illuminant spectra. In the second part of this study we illustrate a new method to reconstruct the illuminant spectra from many locations within an image using the red/green/blue (RGB) values of single pixels within images of a white cardboard sheet acquired by a digital video (DV) camera in forests.

2. METHODS

A. Collection of Illuminant Spectra

Natural illuminant spectra of a total of 238 samples were collected in the temperate forests of several state parks of Maryland (including Patapsco, Greenbelt, and Cunningham) in July and August of 1999. Illuminant spectra were measured at different times of the day (from sunrise to sunset), at various locations (including forest shade, woodland shade, small gaps, and large gaps; see Ref. 7 for

details), and under different weather conditions (sunny and cloudy days). Measurements were made with an Ocean Optics S2000 spectroradiometer calibrated with a standard light source (LS1CAL, Ocean Optics). The S2000 has spectral resolution of 3 nm (the full width at half-maximum). The optic fiber used was 200 μm in diameter and 15 m in length. Light was collected with a cosine collector (Ocean Optics) in front of the optic fiber. All illuminant spectra were measured in quantum units between 400 and 700 nm, smoothed with a Gaussian filter (standard deviation 2 nm) and sampled at 1-nm intervals. All data are available at the following web site: http://umbc7.umbc.edu/~cronin/forest_illuminant.html.

B. Collection of Illuminant Images

A white cardboard square (20 × 20 cm, code 3X.32, Crescent Cardboard Co.) was held at a 45° angle, 75 cm above the forest floor. Images of this square, which represent the distribution of the illuminants falling on it, were recorded by a Sony DV camera (DCR-VX1000) at the same height as the white cardboard. To make sure that the illuminant spectra measured by the S2000 and the illuminant images recorded by the DV camera corresponded, we mounted the cosine collector in the center of white cardboard at the same angle (45° vertically) and collected data sets simultaneously. We also chose locations in which the illuminant was distributed as evenly as possible over the surface of the cardboard, as visualized by eye. The reflectance spectrum of the white cardboard was measured with an Ocean Optics S2000 spectroradiometer with reference to a 100% diffuse white reflectance standard (Spectralon, Labsphere). The reflectance of the white cardboard is generally flat across the spectral range, except for the very short wavelength end [Fig. 1(a), solid curve]. The angular reflectance function of the white cardboard was examined by setting a light source at 90° of elevation and measuring the reflectance between 90° and 10° of elevation. The surface of the white cardboard is reasonably uniform and approximately Lambertian [Fig. 1(b)]. The spectral sensitivity functions of all three CCD chips (RGB) of the DV camera were measured in the laboratory with a monochromator and a calibrated Ocean Optics S2000 spectroradiometer [Fig. 1(a), dashed curves]. The DV camera was set up as follows: shutter speed, 1/125 s; white balance, outdoor mode. Apertures tested were f1.8, f2.8, f4, f5.6, f8, and f11. We minimized any potential nonlinearity of the CCD for the extremes of the intensity range by analyzing only the image whose minimum and maximum intensities in all three channels were greater than 30 levels but less than 220 levels, of a possible total of 256 levels.

C. Principal-Component Analysis

The method of principal-component analysis (PCA) follows that of Judd *et al.*[1] Illuminant spectra were normalized to their spectral values at 560 nm. Then the mean spectrum was subtracted from all the spectra, and a set of orthonormal principal components was found with Simonds's algorithm.[8] The spectra were approximated as

$$S_N(\lambda) = S_0(\lambda) + \sum_{i=1}^{N} M_i V_i(\lambda), \tag{1}$$

where λ denotes wavelength, $S_N(\lambda)$ is the approximated illuminant spectrum with use of N principal components, $S_0(\lambda)$ is the mean spectrum, M_i is the scalar multiple or weight for the ith PC, and $V_i(\lambda)$ is the ith PC or basis function.

For each spectrum, the error of approximation was calculated as

$$Er = \sqrt{\int_{400}^{700} [S(\lambda) - S_N(\lambda)]^2 d\lambda / L}, \tag{2}$$

where Er is the root-mean-square error, $S(\lambda)$ is the actual measurement of the illuminant spectrum, $S_N(\lambda)$ is the approximated spectrum, and L is the length of the interval over which the integration is performed (300 nm in this study).

D. Reconstruction of Illuminant Spectra

The method of reconstruction of illuminant spectra is modified from that used by Vorobyev[9] and Vorobyev *et al.*[10] for reconstruction of reflectance spectra. Here we reconstructed illumination spectra from the DV camera measurements using a least-squares procedure. This

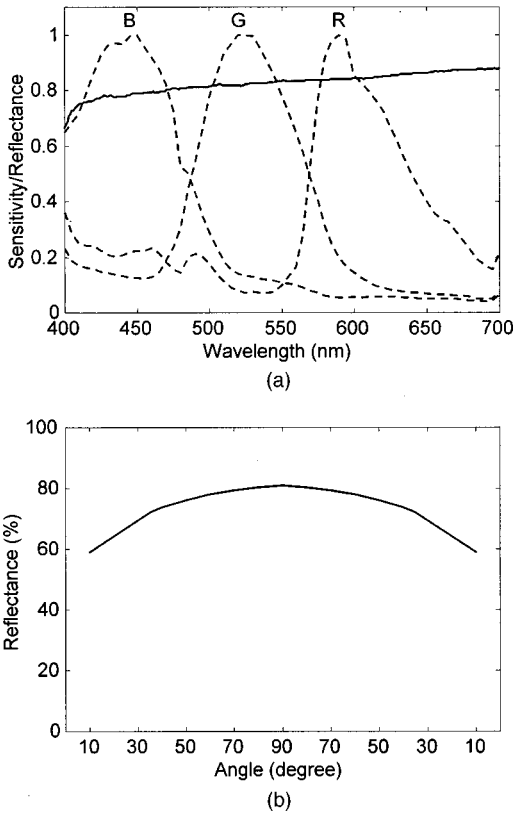

Fig. 1. (a) Normalized spectral sensitivity functions of RGB channels of our Sony DCR-VX1000 DV camera (dashed curves), together with the reflectance spectrum of the white cardboard (solid curve) used as a standard in this study. (b) Angular reflectance function of the white cardboard. The light source was set at 90° elevation, and reflectance was measured between 90° and 10° elevation. This plot gives reflectance at a wavelength of 550 nm, but the curve is similar for all other wavelengths.

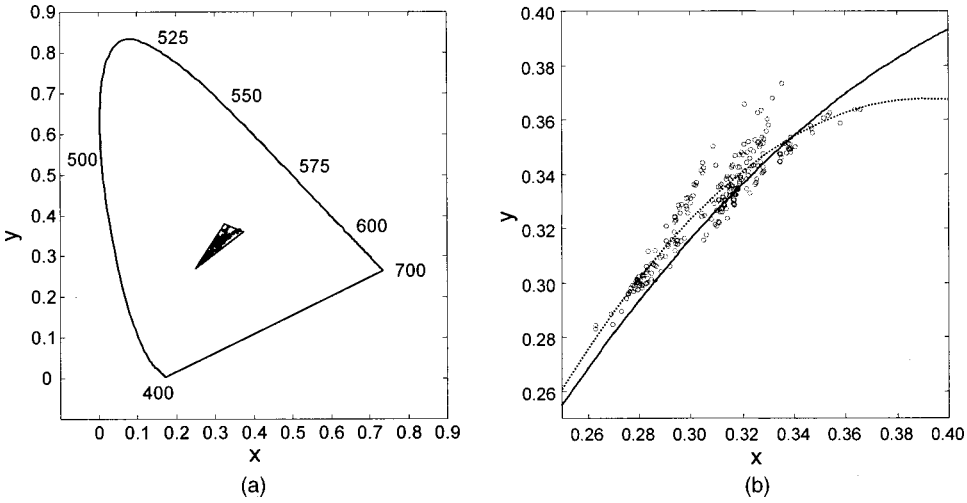

Fig. 2. Chromaticities of 238 natural illuminants measured in forests. The chromaticity diagram is based on CIE (1931) color matching functions. (a) The overall chromaticity diagram. All illuminant spectra lie near the center of the diagram. The loci are constrained by a triangle with vertices at (0.250, 0.270), (0.325, 0.380), and (0.375, 0.360). (b) The central portion of the chromaticity diagram. The solid curve indicates the approximate loci of daylight spectra derived from Judd *et al.*[1] ($y = 2.870x - 3.000x^2 - 0.275$). The dotted curve represents the quadratic regression line ($y = 4.226x - 5.411x^2 - 0.458$) that approximates loci of our forest illuminant spectra.

method is based on direct estimation of the spectra rather than on the estimation of the principal components. Each RGB triplet from the average of the central 50 × 50 pixels of the white cardboard image (excluding the central area occupied by the cosine collector of the S2000) was normalized to its R value. Consequently, the data obtained with the DV camera are described by a two-dimensional vector (G/R, B/R), denoted $\mathbf{q}$. Each illuminant spectrum (ranging from 400 to 700 nm, at 1 nm intervals) corresponding to each RGB triplet was normalized to its spectral value at λ_{560}. Thus the illuminant is described by a 301-dimensional vector, denoted $\mathbf{z}$. Our goal was to find a linear transformation $\bar{\mathbf{B}}$ that maps the two-dimensional vector $\mathbf{q}$ onto the 301-dimensional vector $\mathbf{z}$ such that the mean error is minimal. Using vector notation we can rewrite the equation for the mean error [Eq. (2)] as

$$Er^2 = \langle |\mathbf{z} - \bar{\mathbf{B}}\,\mathbf{q}|^2 \rangle = \langle (\mathbf{z} - \bar{\mathbf{B}}\,\mathbf{q}) \cdot (\mathbf{z} - \bar{\mathbf{B}}\,\mathbf{q}) \rangle, \quad (3)$$

where the dot denotes the inner product, i.e., the sum or the integral of the products of components of two vectors, and $\langle ... \rangle$ denotes the average over the illuminant spectra and division by the length of the interval L over which the integration is performed. Equation (3) defines an error of approximation as a function of a matrix $\bar{\mathbf{B}}$. In general, a minimum (or a maximum) of a function can be found from the condition that the first derivative of a function is equal to zero. This method is well known for functions of scalar variables. The same method is also valid in the case of functions of matrices.[11] For the sake of simplicity we subtract from each illuminant spectrum the mean illuminant spectrum taken over all data $\mathbf{z}_0$ and from each DV camera measurement the mean value, $\mathbf{q}_0$. We denote $\mathbf{z} - \mathbf{z}_0$ as $\mathbf{z}^c$ and $\mathbf{q} - \mathbf{q}_0$ as $\mathbf{q}^c$; then Eq. (3) can be rewritten as

$$Er^2 = \langle \mathbf{z}^c \cdot \mathbf{z}^c - 2\bar{\mathbf{B}}\mathbf{q}^c \cdot \mathbf{z}^c + \bar{\mathbf{B}}\mathbf{q}^c \cdot \bar{\mathbf{B}}\mathbf{q}^c \rangle. \quad (4)$$

To find a derivative of Er^2, we rewrite Eq. (4) in matrix notation using common properties of the inner product:

$$Er^2 = \mathrm{Tr}(\langle \mathbf{z}^c \times \mathbf{z}^c \rangle - \langle \mathbf{q}^c \times \mathbf{z}^c \rangle^T \bar{\mathbf{B}}^T - \bar{\mathbf{B}}\langle \mathbf{q}^c \times \mathbf{z}^c \rangle + \bar{\mathbf{B}}\langle \mathbf{q}^c \times \mathbf{q}^c \rangle \bar{\mathbf{B}}^T), \quad (5)$$

where Tr denotes the trace (i.e., the sum of diagonal entries of a square matrix), index T denotes the transpose, × denotes a direct product of the vectors (i.e., $\langle \mathbf{q}^c \times \mathbf{q}^c \rangle$ is a matrix with the elements $\langle \mathbf{q}^c_i \mathbf{q}^c_k \rangle$; $\langle \mathbf{z}^c \times \mathbf{z}^c \rangle$ is a function of two variables, λ_1 and λ_2, given by $\langle \mathbf{z}^c(\lambda_1)\mathbf{z}^c(\lambda_2) \rangle$; $\langle \mathbf{q}^c \times \mathbf{z}^c \rangle$ is given by 2 functions $\langle \mathbf{q}^c_i \mathbf{z}^c(\lambda) \rangle$). The rules of differentiating functions of matrixes are similar to those for functions of scalars.[11] An application of these rules gives

$$\mathrm{d}(Er^2)/\mathrm{d}\bar{\mathbf{B}}^T = 2[-\langle \mathbf{q}^c \times \mathbf{z}^c \rangle^T + \bar{\mathbf{B}}\langle \mathbf{q}^c \times \mathbf{q}^c \rangle]. \quad (6)$$

To find a solution of the equation $\mathrm{d}(Er^2)/\mathrm{d}\bar{\mathbf{B}}^T = 0$, we multiply Eq. (6) on the right-hand side by $\langle \mathbf{q}^c \times \mathbf{q}^c \rangle^{-1}$. This gives the following expression for the transformation matrix $\bar{\mathbf{B}}$:

$$\bar{\mathbf{B}} = \langle \mathbf{q}^c \times \mathbf{z}^c \rangle^T \langle \mathbf{q}^c \times \mathbf{q}^c \rangle^{-1}. \quad (7)$$

Thus the approximated illuminant spectrum, $\mathbf{z}_{\mathrm{approx}}$, can be written as

$$\mathbf{z}_{\mathrm{approx}} = \bar{\mathbf{B}}\mathbf{q}^c + \mathbf{z}_0, \quad (8)$$

where the matrix $\bar{\mathbf{B}}$ is given by Eq. (7).

3. RESULTS

A. Characterization of Forest Illuminant Spectra

The chromaticity loci of 238 natural illuminant spectra measured in forests are plotted in the CIE 1931 chromaticity diagram (Fig. 2). The loci are constrained by a triangle with vertices at (0.250, 0.270), (0.325, 0.380), and (0.375, 0.360) [Fig. 2(a)]. The loci of 622 daylight spectra used by Judd *et al.*[1] in their Fig. 2 lie nicely on the curve given by $y = 2.870x - 3.000x^2 - 0.275$ [solid curve in

Fig. 2(b) here]. On the basis of this observation, Judd *et al.*[1] proposed that daylight could be described with only one parameter, namely the color temperature. In comparison with the loci of the daylight spectra,[1] the loci of our forest illuminant spectra tend to trail off toward the green side of this diagram [Fig. 2(b)]. Quadratic regression reveals that the dependence between the coordinates of the chromaticity diagram is given by $y = 4.226x - 5.411x^2 - 0.458$ [dotted curve in Fig. 2(b)], which differs markedly from the curve on which the daylight spectra lie. It is important to note that loci of many forest illuminants, especially of those having greenish colors, deviate from the curve given by regression. Thus colors of forest illuminants cannot be described accurately by only one parameter.

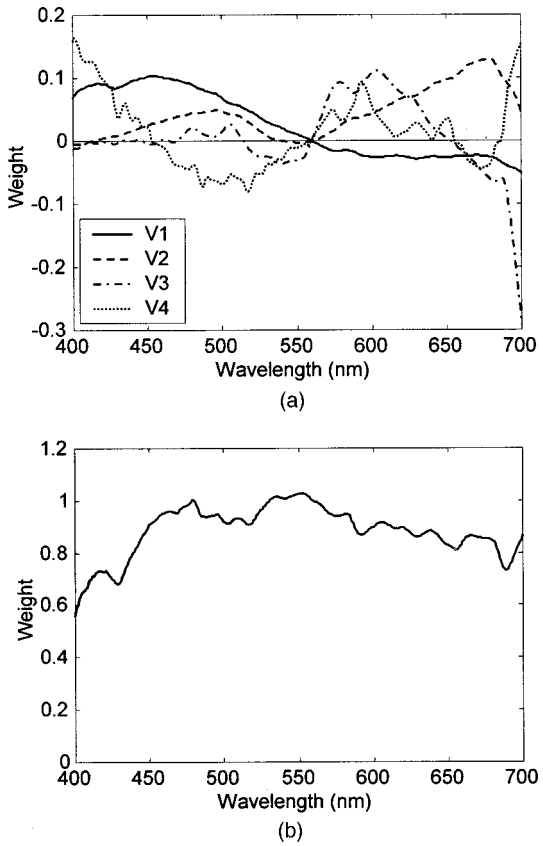

Fig. 3. PCA of 238 forest illuminant spectra. (a) The first four characteristic vectors (principal components) derived from all illuminant spectra measured in forests. Vector 1 (V1, solid curve) explains 65.07% of the total variance, vector 2 (V2, dashed curve) explains 31.88% of the total variance, vector 3 (V3, dotted–dashed curve) explains 1.47% of the total variance, and vector 4 (V4, dotted curve) explains 1.03% of the total variance. (b) The mean spectrum of 238 forest illuminant spectra.

To characterize the spectral properties of natural illuminants in forests, we used PCA, also termed characteristic vector analysis, which is identical to the method Judd *et al.*[1] used to analyze their daylight spectra. The spectra were approximated by a sum of mean and principal components (Fig. 3). The accuracy of the approximation [Eq. (2)], depending on the number of components used, is given in Table 1. As for Judd *et al.*,[1] the forest illuminant spectra can be well approximated by two characteristic vectors (Fig. 4 and Table 1).

B. Relation between Scalar Multiples and Chromaticity Coordinates

In the case of forest light, the spectrum of illumination can be predicted from its chromaticity coordinates (x, y), because forest illuminants can be approximated with high accuracy by two parameters, M_1 and M_2 (Fig. 4). To find a map of M_1 and M_2 onto (x, y), and of (x, y) onto M_1 and M_2, we use the method described by Judd *et al.*[1] Any spectrum reconstructed from a mean and two scalar multiples is computed as [see Eq. (1)]

$$S_{\text{approx}}(\lambda) = S_0(\lambda) + M_1 V_1(\lambda) + M_2 V_2(\lambda), \qquad (9)$$

and the tristimulus value $\mathbf{X}$ of the spectrum can be written as

$$\mathbf{X} = \int_{400}^{700} S_{\text{approx}}(\lambda)\mathbf{x}(\lambda)\mathrm{d}\lambda = \int_{400}^{700} [S_0(\lambda) + M_1 V_1(\lambda) + M_2 V_2(\lambda)]\mathbf{x}(\lambda)\mathrm{d}\lambda, \qquad (10)$$

where the $\mathbf{x}(\lambda)$ is one of the color matching functions of the 1931 CIE standard observer for colorimetry.[6] Note that we performed PCA with spectra recorded in quantum units. Thus the color matching functions were converted from energy units into quantum units. Since the scalar multiples M_1 and M_2 are constants independent of

Table 1. Errors of the Estimation of Forest Illuminant Spectra Based on the Different Linear Combinations of the Mean Spectrum and the First Four Principal Components of Forest Illuminants and of Judd *et al.*[a] Daylight Spectra

Number of PC's Used	Mean[b]		1 Quartile		Median		3 Quartile	
	Forest	Judd	Forest	Judd	Forest	Judd	Forest	Judd
Mean Only	0.1371	0.1606	0.0641	0.0931	0.1119	0.1443	0.1555	0.1846
1	0.0815	0.1210	0.0302	0.0543	0.0509	0.0857	0.0888	0.1334
2	0.0208	0.0569	0.0125	0.0259	0.0156	0.0339	0.0220	0.0632
3	0.0149	0.0398	0.0087	0.0225	0.0118	0.0270	0.0155	0.0422
4	0.0082	0.0388	0.0047	0.0208	0.0061	0.0271	0.0082	0.0402

[a] Ref. 1
[b] "Mean" is the average root-mean-square difference of the spectra.

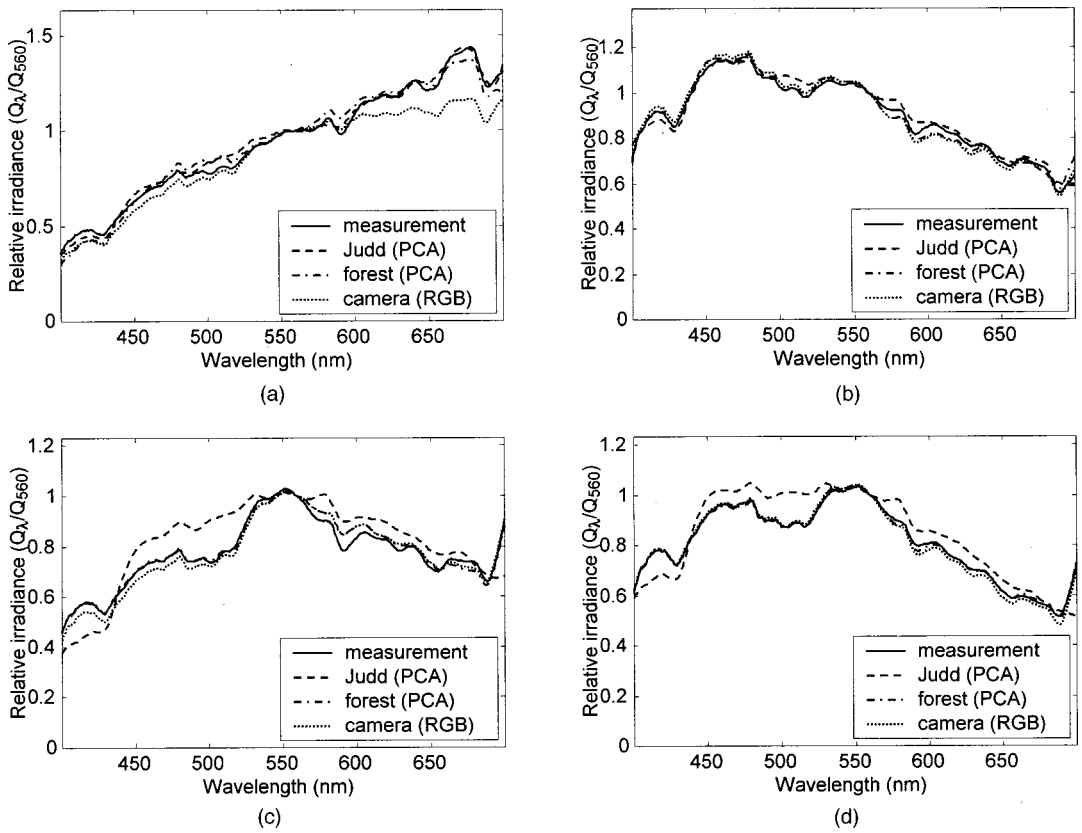

Fig. 4. Approximation of forest illuminant spectra. Solid curves, illuminant spectrum measured by the S2000 spectroradiometer normalized to the spectral value at 560 nm. Dotted–dashed curves, reconstructed illuminant spectrum based on the linear combination of the first two principal components and the mean spectrum. Dashed curves, forest illuminant spectra approximated with the first two PCs of Judd *et al.*[1] Dotted curves, illuminant spectrum reconstructed from the RGB values in the DV images of the white cardboard square. The spectrum is selected to represent a typical forest spectrum from one of four classes: (a) sunlight, (b) skylight, (c) green light shining through leaves, (d) a mixture of skylight and green light.

wavelength for any reconstructed curve, the expression for X can be rewritten as

$$X = X_0 + M_1X_1 + M_2X_2, \tag{11a}$$

where X_0 is the X-tristimulus value of the mean spectrum, and X_1 and X_2 are the X-tristimulus values of the two characteristic vectors; for example, $X_1 = \int_{400}^{700} V_1(\lambda) \cdot x(\lambda)\mathrm{d}\lambda$. Analogous expressions are valid for Y and Z components:

$$Y = Y_0 + M_1Y_1 + M_2Y_2, \tag{11b}$$

$$Z = Z_0 + M_1Z_1 + M_2Z_2. \tag{11c}$$

The connection between scalar multiples M_1 and M_2, and chromaticity coordinates (x, y) follows directly from Eqs. (11) and from definitions: $x = X/(X + Y + Z)$, $y = Y/(X + Y + Z)$. A convenient form of connection, for $X + Y + Z$ abbreviated as S, is

$$x = \frac{X_0/S_0 + M_1X_1/S_0 + M_2X_2/S_0}{1 + M_1S_1/S_0 + M_2S_2/S_0},$$

$$y = \frac{Y_0/S_0 + M_1Y_1/S_0 + M_2Y_2/S_0}{1 + M_1S_1/S_0 + M_2S_2/S_0}. \tag{12}$$

To find the scalar multiples M_1 and M_2 required to yield a reconstructed spectrum of an illuminant having any arbitrarily chosen values x and y of chromaticity coordinates, it is necessary to solve for M_1 and M_2 from Eqs. (12). This solution is given by the following equations:

$$M_1 = \frac{X_0Y_2 - X_2Y_0 + (Y_0S_2 - Y_2S_0)x + (X_2S_0 - X_0S_2)y}{X_2Y_1 - X_1Y_2 + (Y_2S_1 - Y_1S_2)x + (X_1S_2 - X_2S_1)y},$$

$$M_2 = \frac{X_1Y_0 - X_0Y_1 + (Y_1S_0 - Y_0S_1)x + (X_0S_1 - X_1S_0)y}{X_2Y_1 - X_1Y_2 + (Y_2S_1 - Y_1S_2)x + (X_1S_2 - X_2S_1)y}. \tag{13}$$

The tristimulus values of mean and of the first two characteristic vectors have been calculated and found to be as follows: $X_0 = 95.8557$, $Y_0 = 102.154$, $Z_0 = 113.802$, $X_1 = 0.796038$, $Y_1 = 1.18499$, $Z_1 = 12.1479$, $X_2 = 3.91398$, $Y_2 = 2.70927$, $Z_2 = 3.26635$. Substitution of these tristimulus values into Eqs. (12) and (13) yields

$$x = \frac{0.30742 + 0.00255M_1 + 0.01255M_2}{1.00000 + 0.04531M_1 + 0.03172M_2},$$

$$y = \frac{0.32276 + 0.00380M_1 + 0.00869M_2}{1.00000 + 0.04531M_1 + 0.03172M_2}, \quad (14)$$

$$M_1 = \frac{-140.1297 + 165.4801x + 272.4502y}{2.4813 + 26.5600x - 47.4278y},$$

$$M_2 = \frac{-32.2696 - 1073.8x + 1106.1y}{2.4813 + 26.5600x - 47.4278y}. \quad (15)$$

C. Comparison between Forest Illuminant Spectra and Standard Daylight Spectra

To quantify the differences between our forest illuminant spectra and the standard daylight spectra of Judd *et al.*,[1] we consider two methods: (i) comparison of the span of the subspaces of principal components derived from both sets of illuminant spectra and (ii) comparison of the accuracy of forest illuminant spectra approximated by principal components of Judd *et al.*[1] with the accuracy of our approximations.

It is important to note that Judd *et al.*[1] used energy units in describing their daylight spectra, whereas we used quantum units in describing our forest illuminant spectra. Because visual processing starts with photon detection, the use of quantum units has direct benefits in vision research.[12,13] To make the results comparable, we converted our forest illuminant spectra into energy units and repeated the PCA (Fig. 5). Furthermore, Judd *et al.*[1] analyzed their daylight spectra in the spectral range from 300 to 830 nm. Thus their principal components are not orthogonal in the spectral range used in the present study (400–700 nm). We orthogonalized the principal components of their standard daylight spectra using a Gramm–Schmidt algorithm[11] (Fig. 5). This method leaves the first principal component invariant. Then a function that is orthogonal to the first principal component can be found as a linear combination of the first and second principal components. This procedure is repeated for further principal components. For any given number of basis functions, the Gramm–Schmidt algorithm does not alter the space spanned by these basis functions; rather, it only changes the coordinate system.

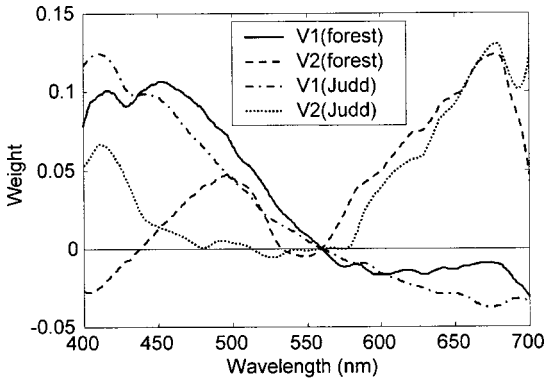

Fig. 5. Comparison of the first two principal components of our 238 forest illuminant spectra (in energy units) and 622 daylight spectra of Judd *et al.*[1] (in energy units).

Table 2. Distances between the Subspaces Spanned by Basis Functions of Forest Illuminant Spectra and Judd *et al.*[a] Daylight Spectra[b]

Number of Basis Functions Used	1	2	3	4
Distance	0.1779	0.5494	0.4049	0.9060

[a] Ref. 1.
[b] See Appendix A for details.

Let F_n be a subspace defined by n basis functions of our forest illuminant spectra, and D_n be the subspace of n basis functions of the standard daylight spectra of Judd *et al.*[1] The fact that the basis functions of the two subspaces differ substantially does not necessarily mean that the two subspaces are different. If the basis functions of F_n can be represented as a linear combination of those of D_n, then the two subspaces are identical. Thus the inspection of basis functions themselves does not allow us to conclude whether the two subspaces are different. To compare the subspaces rather than their basis functions, we use the following method.

Generally, the larger the distance between vectors in these subspaces, the more different the subspaces are. The distance between the vectors depends on their length and orientation. To quantify the distance between subspaces, we consider a distance d of a unit vector in F_n, a to its projection onto D_n, a_D. If a belongs to both subspaces F_n and D_n, then $a = a_D$ and $d = 0$. If a is orthogonal to a_D, then $d = 1$. The magnitude of the maximum of d over the orientations of a, d_{max}, gives the measure of the difference between F_n and D_n. In the case of two planes (two-dimensional subspaces of a three-dimensional space), d_{max} is equal to the sine of the angle between the planes. The method for finding d_{max} is given in Appendix A. Note that the value of d_{max} does not depend on whether the distance between the vector in F_n and its projection onto D_n or between the vector in D_n and its projection onto F_n is considered (see Appendix A). Table 2 gives the results of the comparison. The first components are similar to each other, and the subspaces given by two and by three components differ by 0.54 and by 0.4 of the maximum value of 1, respectively. When four-dimensional subspaces are compared, the distance approaches 1. This result indicates that the subspaces of the two sets of illuminant spectra differ significantly.

The alternative way to compare our forest illuminant spectra and the daylight spectra of Judd *et al.*[1] is to examine the accuracy of approximated forest illuminant spectra by using the principal components of Judd *et al.*[1] derived from their daylight spectra. If both sets of spectra were similar, one would expect that the approximation of forest illuminant spectra using the principal components of Judd *et al.*[1] will give a fairly high accuracy. We illustrate the differences in the accuracy of reconstruction by two sets of principal components, using four typical forest illuminant spectra. They were selected to represent direct sunlight [Fig. 4(a)], skylight from a clear blue sky [Fig. 4(b)], green light shining through leaves [Fig. 4(c)], and a mixture of skylight and green light [Fig. 4(d)]. Sunlight and clear blue sky can be approximated nicely by the first two principal components of Judd *et al.*[1]

(Fig. 4, upper row). However, if the spectra have a 550-nm hump (Fig. 4, lower row), corresponding to the filtering effects of leaves, then the approximation using the first two principal components of Judd *et al.*[1] fails to reconstruct the illuminant spectra. The error of approximation for all 238 forest illuminant spectra by the principal components of Judd *et al.*[1] is given in Table 1.

D. Reconstruction of Forest Illuminant Spectra From the RGB Values

We find that it is possible to map accurately the lower-dimensional RGB values of the white cardboard images to the higher-dimensional spectra of the illuminants. This is because (i) natural illuminants in forests are nicely fitted with two characteristic vectors and the mean spectrum (Table 1 and Fig. 4); (ii) the spectral sensitivity functions of the three CCD chips of the DV camera have broadband sensitivities, with λ_{max} at 450, 520, and 585 nm for B, G, and R channels, respectively [Fig. 1(a), dashed curves]; and (iii) the reflectance spectrum of the white cardboard is reasonably flat across the visible range [Fig. 1(a), solid curve]. Also, reflectance from the white cardboard represents all illumination falling on each point of its surface reasonably accurately because its surface is approximately Lambertian [Fig. 1(b)].

With Eq. (7), we computed the transformation matrix $\bar{\mathbf{B}}$ by using 238 RGB triplets of images of the white cardboard paired with 238 illuminant spectra. To reconstruct each illuminant spectrum from the RGB triplet, Eq. (8) was used. Figure 3(b) shows the mean illuminant spectrum, $\mathbf{z}_0$; Fig. 6 shows the two vectors of transformation matrix, $\bar{\mathbf{B}}$; and the values for $\mathbf{q}_0$ are 1.0873 and 0.9880 for G/R and B/R, respectively. Overall, the approximated illuminant spectra (Fig. 4, dotted curves) fitted by a linear least-squares-fit estimation are very close to the measured spectra (Fig. 4, solid curves). This approximation is accurate for all 238 forest illuminant spectra. The error of the estimation of forest illuminant spectra based on the direct transformation of RGB values derived in this study is shown in Table 3.

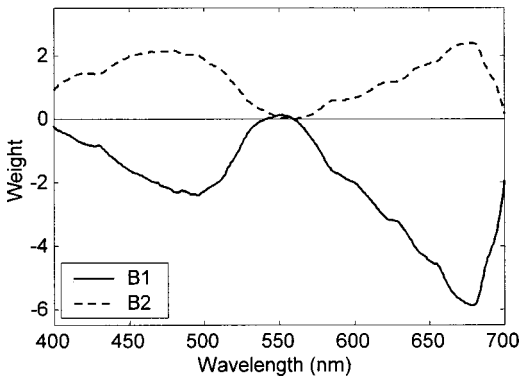

Fig. 6. Two vectors of the transformation matrix $\bar{\mathbf{B}}$. Vector B1 (solid curve) corresponds to the G/R value, and vector B2 (dashed curve) corresponds to the B/R value in Eq. (8) (see text for details).

Table 3. Errors of the Estimation of Forest Illuminant Spectra Based on the Direct Transformation of RGB Values Derived in This Study

Mean[a]	1 Quartile	Median	3 Quartile
0.0599	0.0301	0.0428	0.0582

[a] "Mean" is the average root-mean-square difference of the spectra.

Reconstruction from the camera data is inevitably less accurate than reconstruction from the principal components. Two factors limit the accuracy of reconstruction. First, the measurements are noisy. Second, the spectral sensitivities of the RGB channels are not ideally fitted to the principal components (i.e., they also receive inputs from the principal components of higher orders). It is interesting to compare a two-dimensional subspace defined by a transformation matrix $\bar{\mathbf{B}}$ with the subspace of the first two principal components of forest illuminants. If the subspace of $\bar{\mathbf{B}}$ is similar to the subspace of the first two principal components, we can conclude that the sensitivities of camera do not receive significant input from the higher-order components. Calculations show that the distance between the subspaces is only 0.044 of the maximum value of 1, which indicates that the sensitivities of camera are well suited for the measurements of illuminant spectra.

4. DISCUSSION

Illumination in forests is potentially more complex than that in open terrains.[7] In addition to regions illuminated by direct sunlight or in the shadow of opaque objects, many regions in forests are illuminated by light filtered through foliage. The illumination spectrum depends, therefore, on the physical structure of the forest (whether it is a rainforest or temperate woodland), on the species of trees present and the time of year, and on the location in the forest. Endler[7] recognized the importance of variations in illumination to forest biology. He collected diverse light spectra in forests worldwide and defined five different categories of spectra: forest shade, woodland shade, small gaps, large gaps, and dawn/dusk. Our 238 forest illuminant spectra can readily be assigned to Endler's categories. By doing PCA on these forest illuminant spectra, we can proceed to describe the spectral properties of illuminants in forests and to compare them with the spectral properties of daylight characterized earlier by Judd *et al.*[1]

In general, forest illuminant spectra, like the daylight spectra of Judd *et al.*,[1] can be accurately approximated with only two characteristic vectors and the mean spectrum (Fig. 4, dotted–dashed curves). There are two important differences between forest and daylight illuminants. First, the chromaticity loci of forest illuminants deviate to the green from the loci of daylights, and unlike the daylight spectra the forest spectra cannot be accurately described by one parameter. Second, low-dimensional subspaces of forest spectra differ from those of daylight, and as a result the accuracy of approximation of forest spectra by principal components derived from daylight spectra is poor compared with the accuracy of approximation of forest spectra by their own principal components. These results point to a fundamental difference between forest illuminants and skylight in open terrain.

We also derived a formal connection between the scalar multiples and the chromaticity coordinates of our forest illuminant spectra, as Judd *et al.*[1] did for their daylight spectra. These expressions provide a convenient way to access the forest illuminant spectra for colorimetric application.

In the second part of this study we illustrated a method to reconstruct illuminant spectra directly from the RGB values of a white cardboard image acquired from the DV camera. Linear methods of approximation of spectral data are widely used, and different tasks require different models.[14,15] Marimont and Wandell[15] developed a method of linear approximation of reflectance spectra that minimizes the reconstruction error of sensor responses. In this case it was assumed that the spectra were known, and the goal was to develop the most economical representation. To find the best linear model, Marimont and Wandell used a least-squares method. We also used a least-squares method, but our task was different. We reconstructed the illuminant spectra, given that the responses of the sensors were known. Theoretically, the best possible linear approximation with the minimal number of parameters is achieved by principal components. In reality, it is impossible to achieve the same accuracy if spectra are reconstructed from a limited number of measurements, because the measurements are noisy and sensors are not ideally tuned to the set of spectra. We showed that the functions used for reconstruction of the illuminant from the RGB data are close (but not identical) to the subspace of the first two principal components, which indicates that the spectral sensitivities of RGB channels of the DV camera are well suited for the reconstruction of forest illuminations.

We used an empirical relation between the RGB data and the illumination data and found a linear algorithm that minimizes the error of approximation. This method gives the best performance for the given sensitivities of the RGB channels and the accuracy of measurements. Previously, a similar algorithm of reconstruction had been derived by theoretical calculations based on statistics of spectra given by PCA and on the shapes of the spectral sensitivities of spectral channels.[9,10] Whereas Vorobyev *et al.*[9,10] approximated the spectra on absolute scale, we considered the spectra normalized to unity at 560 nm. This implies that we had to exclude the intensity domain from the measurements before using them for approximation. We did this by dividing each of the RGB triplet values by its R value. That is, a division (a nonlinear transformation) was applied both to the spectra and to the RGB data before mapping of one data set to another was found. Nevertheless, a linear transformation accurately related the RGB data to spectra. This provides an economical method for measurements of spatial and temporal variations of illumination.

APPENDIX A

Consider n-dimensional subspaces F_n and D_n. Let $\mathbf{a}$ be a unity vector in the subspace F_n and $\mathbf{a}_D$ be a projection of $\mathbf{a}$ onto D_n. The distance d between $\mathbf{a}$ and $\mathbf{a}_D$ is defined as

$$d^2 = \|\mathbf{a} - \mathbf{a}_D\|^2 = (\mathbf{a} - \mathbf{a}_D) \cdot (\mathbf{a} - \mathbf{a}_D) = \mathbf{a}^2 - 2\mathbf{a}_D \cdot \mathbf{a} + \mathbf{a}_D{}^2. \quad \text{(A1)}$$

From a definition of projection, it follows that $\mathbf{a}_D \cdot \mathbf{a} = \mathbf{a}_D{}^2$, and $\mathbf{a}^2 = 1$, because we defined $\mathbf{a}$ as a unity vector. Thus

$$d^2 = 1 - \mathbf{a}_D{}^2. \quad \text{(A2)}$$

Our goal is to find a maximum of d over all possible orientations of $\mathbf{a}$. This maximum is reached when $\mathbf{a}_D$ is minimal.

We express $\mathbf{a}$ in the coordinate frame of orthonormal basis vectors of F_n, $\mathbf{u}_n$ and express $\mathbf{a}_D$ in the coordinate frame of orthonormal basis vectors of D_n, $\mathbf{v}_n$:

$$\mathbf{a} = \sum_{k=1}^{n} a^k \mathbf{u}_k, \quad \text{(A3)}$$

where a^k is a projection of $\mathbf{a}$ onto $\mathbf{u}_k$. Similarly,

$$a_D = \sum_{i=1}^{n} a_D{}^i \mathbf{v}_i, \quad \text{(A4)}$$

where $a_D{}^i$ is a projection of $\mathbf{a}$ onto $\mathbf{v}_i$. Note that $a_D{}^i = \mathbf{a}\mathbf{v}_i$. Substitution of Eq. (A3) into Eq. (A4) gives

$$\mathbf{a}_D = \sum_{k=1}^{n} \sum_{i=1}^{n} a^k (\mathbf{u}_k \cdot \mathbf{v}_i) \mathbf{v}_i. \quad \text{(A5)}$$

Thus

$$\mathbf{a}_D{}^2 = \sum_{k=1}^{n} \sum_{i=1}^{n} \sum_{j=1}^{n} a^k (\mathbf{u}_k \cdot \mathbf{v}_i)(\mathbf{u}_j \cdot \mathbf{v}_i) a^j. \quad \text{(A6)}$$

Let $\mathbf{W}$ be a matrix with the elements $(\mathbf{u}_k \cdot \mathbf{v}_i)$. Then we can rewrite Eq. (A6) as

$$\mathbf{a}_D{}^2 = \mathbf{a}\ \mathbf{W}\ \mathbf{W}^T\mathbf{a} = \mathbf{a}\ \mathbf{M}\ \mathbf{a}, \quad \text{(A7)}$$

where index T denotes transpose and $\mathbf{M} = \mathbf{W}\ \mathbf{W}^T$. Because $\mathbf{M}$ is a symmetrical matrix, it can be transformed to diagonal form by a rotation of the coordinate frame. In this new coordinate system, Eq. (A7) can be rewritten as

$$\mathbf{a}_D{}^2 = \sum_{k=1}^{n} (\tilde{a}^k)^2 L_k, \quad \text{(A8)}$$

where L_k denotes the eigenvalues of $\mathbf{M}$ and $\tilde{a}^k$ denotes the coordinates of vector $\mathbf{a}$ in the new coordinate frame. Because $\mathbf{a}$ is a unity vector, $\Sigma(\tilde{a}^k)^2 = 1$. It is easy to see that $\mathbf{a}_D{}^2$ reaches its minimum when $\mathbf{a}$ is parallel to the coordinate axes corresponding to the minimal of eigenvalues. In this case, one of $\tilde{a}^k$ is equal to unity, while others are equal to zero. Thus the minimum of $\mathbf{a}_D{}^2$,

$$(\mathbf{a}_D{}^2)_{\min} = L_{\min}, \quad \text{(A9)}$$

where $L_{\min}$ denotes the minimal eigenvalue of matrix $\mathbf{M}$. Substitution of Eq. (A9) into Eq. (A2) gives the following expression for the maximal distance:

$$d_{\max} = \sqrt{(1 - L_{\min})}. \quad \text{(A10)}$$

ACKNOWLEDGMENTS

We acknowledge the assistance of Li-Ching Wang in collecting illuminant and image data in the field. We also thank Dan Ruderman for suggesting the consideration of the distance between the vectors to evaluate the difference between subspaces. This work is based on research supported by National Science Foundation grant IBN-9724028 (to T. W. Cronin).

The corresponding author, Chuan-Chin Chiao, can be reached at his present address, Howard Hughes Medical Institute, 50 Blossom Street, Wellman 429, Massachusetts General Hospital, Boston, Massachusetts 02114, or by phone, 617-726-3888; or e-mail, chiao@umbc7.umbc.edu.

REFERENCES

1. D. B. Judd, D. L. MacAdam, and G. Wyszecki, "Spectral distribution of typical daylight as a function of correlated color temperature," J. Opt. Soc. Am. **54**, 1031–1040 (1964).
2. J. Cohen, "Dependency of the spectral reflectance curves of munsell color chips," Psychon. Sci. **1**, 369–370 (1964).
3. L. T. Maloney, "Evaluation of linear models of surface spectral reflectance with small numbers of parameters," J. Opt. Soc. Am. A **3**, 1673–1683 (1986).
4. J. P. S. Parkkinen, J. Hallikainen, and T. Jaaskelainen, "Characteristic spectra of Munsell colors," J. Opt. Soc. Am. A **6**, 318–322 (1989).
5. M. J. Vrhel, R. Gershon, and L. S. Iwan, "Measurement and analysis of object reflectance spectra," Color Res. Appl. **19**, 4–9 (1994).
6. G. Wyszecki and W. S. Stiles, *Color Sciences: Concepts and Methods, Quantitative Data and Formulae*, 2nd ed. (Wiley, New York, 1982).
7. J. A. Endler, "The color of light in forests and its implications," Ecol. Monogr. **63**, 1–27 (1993).
8. J. L. Simonds, "Application of characteristic vector analysis to photographic and optical response data," J. Opt. Soc. Am. **53**, 968–974 (1963).
9. M. Vorobyev, "Costs and benefits of increasing the dimensionality of colour vision system," in *Biophysics of Photoreception: Molecular and Phototransductive Events*, C. Tardei-Ferretti, ed. (World Scientific, Singapore, 1997), pp. 280–289.
10. M. Vorobyev, A. Gumbert, J. Kunze, M. Giurfa, and R. Menzel, "Flowers through the insect eyes," Isr. J. Plant Sci. **45**, 93–102 (1997).
11. V. I. Smirnov, *A Course of Higher Mathematics* (Pergamon, New York, 1964), Vol. III, Parts 1 and 2.
12. J. A. Endler, "On the measurement and classification of colour in studies of animal colour patterns," Biol. J. Linnean Soc. **41**, 315–352 (1990).
13. J. N. Lythgoe, *The Ecology of Vision* (Clarendon, Oxford, UK, 1979).
14. D. H. Brainard, B. A. Wandell, and W. B. Cowan, "Black light: how sensors filter spectral variation of the illuminant," IEEE Trans. Biomed. Eng. **36**, 140–149 (1989).
15. D. H. Marimont and B. A. Wandell, "Linear models of surface and illuminant spectra," J. Opt. Soc. Am. A **9**, 1905–1913 (1992).